A Planar 2×2 MIMO Antenna Array for 5G Smartphones

A. K. M. Zakir Hossain[1*], Nurulhalim Bin Hassim[2], W. H. W. Hassan[3], Win Adiyansyah Indra[4]
Centre for Telecommunication Research & Innovation (CeTRI), Fakulti Teknologi Kejuruteraan Elektrik & Elektronik (FTKEE), Universiti Teknikal Malaysia Melaka (UTeM), Melaka

Safarudin Gazali Herawan[5]
Industrial Engineering Department, Faculty of Engineering
Bina Nusantara University, Jakarta
Indonesia 11480

Mohamad Zoinol Abidin Bin Abd. Aziz[6]
Centre for Telecommunication Research & Innovation (CeTRI), Fakulti Kejuruteraan Elektronik & Kej. Komputer (FKEKK), Universiti Teknikal Malaysia Melaka (UTeM)
Melaka

***Abstract*—Here, a planar 2×2 MIMO configuration for the 5G smartphone has been presented. A single element modified planar tree profile shape (MPTPS) antenna is implemented to investigate the suitability in future 5G communication for different sub-6 GHz spectrum band. The size of the single MPTPS antenna is 40 × 25 mm^2. The electronic band gap (EBG) and partial ground plane (PGP) techniques have been utilized to tune this antenna. The antenna works from 2.81 – 7.23 GHz, with a (VSWR < 2) bandwidth of 4.42 GHz that covers all the mid-range sub-6 GHz 5G frequencies. It also has a comparatively good gain of 3.14 dBi, high efficiency of 96% and a bi-directional radiation pattern. The antenna has been implemented in a 145 × 75 mm^2 smartphone mainboard with MIMO configuration using polarization diversity. More than -21.1 dB isolation has been found between different ports. A good gain of as high as 6.59 dBi is observed for the MIMO in the band. Also, as MIMO performance, excellent envelope correlation coefficient of less than 0.0029 and minimum diversity gain of 9.9853 has been observed. The investigation has been further stretched by adding a liquid crystal display (LCD) for radiation performance and a hand phantom to assess the performance in terms of specific absorption rate (SAR). It is observed that the SAR value is as low as 0.887641 at 3.5 GHz. This design will motivate the researcher to develop high performance MIMO arrays for 5G smartphones.**

***Keywords*—MIMO; smartphone antenna; isolation; envelope correlation coefficient; diversity gain; specific absorption rate (SAR)**

I. Introduction

Nowadays, in wireless communication, the latest addition is 5G technology. The emergence of the 5G technology will enable improve connectivity, excellent speed and data rate and these all features will come with a very low latency [1]. In terms of the frequency of operation there are two different band of 5G: Sub-6 GHz (below 6 GHz bands) and the millimeter wave band. The millimeter wave band lays between 24 to 30 GHz in different regions. In the sub 6-GHz 5G band, there few sub bands such as lower band (700 MHz), mid band (3.4 to 3.6 GHz) and high band (4.8–6 GHz) [2]. Different countries from different regions have decided to choose different sub-6 GHz band for their future 5G rollout operation. Due to this shuttle change in the working frequencies, all the necessary hardware related to the base transceiver stations (BTS), handphone/smartphones and other user equipment (UE) need to be redesigned or tuned to fit those chosen frequencies. Among various components of those equipment, the antenna is one of the most significant part of the system. The antenna works as the main gateway for any wireless interface by converting the electrical signal to electromagnetic radiation [3]. So, a good design of antenna would impose less stress on other components such as power amplifiers (PAs), low noise amplifiers (LNAs) and etc. Recently, multiple input multiple output (MIMO) array techniques and configurations for smartphones provide a nice edge to the transmission and reception of the wireless signal, enabling low crosstalk, high signal selectivity and channel capacity [4]. In addition, it inherently comes with a better directivity, enhanced beamforming and beam-steering ability. However, it's still challenging for the designers to design a MIMO antenna array that fits inside a smartphone along with the other circuitry element without harming the performance of the entire system to cover the entire mid-range sub-6 GHz frequency range by still keeping the MIMO performance intact in terms of port isolation, envelope correlation coefficient (ECC), diversity gain (DG), and SAR.

II. Literature Review

Recently, research on 5G MIMO array design has got a lot of attention among the researcher and the design engineers. In [5] the authors have proposed a two element MIMO antenna array that works for the sub-6 GHz bands (3.5 and 4.3 GHz) and also in millimeter wave (mmWave) band from 24 – 38 GHz. The authors here have proposed the planar inverted-F (PIFA) structure for the single antenna element. The results show that the minimum isolation between the ports is -21 dB and the ECC is less than 0.05 throughout all the working frequencies. However, the authors have not performed any SAR analysis. As this antenna is intended to be working in the smartphones, it is a necessary to analyze the exposer around any human tissue.

*Corresponding Author

A four port 2 × 2 MIMO antenna array has been proposed using slotted rectangular shaped antenna element works for 5G new radio (NR) band 77, 78 and 79 which covers 3.3 to 4.2 GHz, 3.3 to 3.8 GHz and 4.4 to 5 GHz respectively (sub-6 GHz middle bands) [6]. The authors used E and L shaped slots in the rectangular planar patch to crate the desired resonant frequency bands and also used novel un-protruded multi-slot (UPMS) to isolate the ports. The results show that the ECC is less than 0.01 and, the isolations between the port 1 & 2 and port 3 & 4 are good below -25 dB. However, based on the results presented its can be seen that the isolation between port 2 & 4 and 1 & 3 it is as high as -15 dB which is not desired also. Another point of this proposal is the authors have not done any SAR analysis which is very important for the implementation of this design in the smartphone. A quad port 2 × 2 MIMO antenna for smartphones has been proposed in [7]. The single antenna element for the MIMO is based on the combination of L-shaped, rectangular shaped and Z-shaped strips. The antenna is designed for 3.5GHz (3.4-3.6 GHz) and 5GHz (4.8-5 GHz) bands for 5G application. The isolation between the ports is found to be larger than -16.5 dB and the ECC is less than 0.01 for this proposal. However, the SAR analysis is still missing in the analysis. One more proposal has been made for four element MIMO base on planar dipole single element antenna for smartphone which works 3.5 and 4.7 GHz sub-6 GHz 5G bands [8]. A thorough SAR analysis in this proposal with head and hand phantom defined in the simulator. The SAR value can been seen for the results are 1.8 W/Kg and 1.7 W/Kg for 3.5GHz and 4.7 GHz respectively for 10g tissue mass. Also, a good ECC of below 0.005 has been observing. However, in terms of the isolation between the ports it can be seen that the isolation, even though within the acceptable range, goes as low as -15 dB.

In [9], the authors have proposed a shared dipole antenna structure for the working frequency NR band 77/78/79. The authors have proposed this eight element array design especially for the laptop application. From the presented results it seen that the mutual coupling between ports as less as -19dB. However, the authors have not disclosed the single element antenna gain. Also, some important MIMO parameters such as ECC, (DG) and etc. are missing which are essential to assess the performance of the proposed design. Another 8 element antenna MIMO array has been proposed [10] for 5G smartphones that works between 3.4 to 3.6 GHz. The authors have proposed the MIMO array which can fit on the side edge of the smartphone and comprises with single monopole structures and the total size of the board is chosen to be 145 × 75 mm^2 structure. The configuration exhibits a good ECC of 0.1 and single element gain around 3.5. However, the minimum isolation between the ports comparatively low, dropping around -12 dB which is undesirable. Similarly, a different 8 element 8×8 MIMO antenna configuration has been proposed in [11] which works for sub-6 GHz frequency region. The single element antenna utilized here is a folded monopole with a dimension of 17.85 × 5 mm^2. The work reveals a good ECC of less than 0.06, the mean effective gain varies between 4.18 to 5.67 dBi and the maximum SAR value reaches 0.941 W/Kg. However, one important parameter, the isolation between the ports is not so high, as it drops to -17 dB between the ports which would degrade the whole system performance. Table I summarize the recent works and also make a comparison with this proposed work.

In this article, a modified tree profile shaped (MPTPS) antenna has been proposed and implemented in a 2 × 2 MIMO configuration for smartphones that has a working bandwidth (BW) 2.81 to 7.23 GHz to cover the entire mid-range sub-6 GHz 5G frequencies. The MIMO antenna has comparatively better isolation between the ports. It has better isolation between ports, superior ECC, DG and SAR values compared with the other existing proposals which would improve the overall performance of the smartphone for 5G communication.

TABLE I. SUMMARY OF THE RECENT WORKS WITH THE PROPOSED WORK

References	Isolation (dB)	ECC	SAR (W/Kg)
[5]	- 21	0.05	na
[6]	- 15	0.01	na
[7]	- 16.5	0.01	na
[8]	- 15	0.005	1.7
[9]	- 19	na	na
[10]	- 12	0.1	na
[11]	- 17	0.06	0.941
Proposed work	**- 21.1**	**0.0022**	**0.887641**

*na = not available

This article is organized as: Section II, Literature Review (where the recent related research has been discussed). Section III, MPTPS antenna and MIMO design (this section includes the thorough elaboration and illustration of the design procedure of a single element MTPS antenna and the MIMO design as well). Section IV, Results and Analysis (in this section a deep discussion and analysis has been done by presenting the relevant responses related to the proposed design) and Section V, Conclusion (the article is concluded here and further aspect of this research has been revealed).

III. MPTPS ANTENNA AND MIMO DESIGN

Fig. 1 comprises the front and back view geometry of the proposed MPTPS antenna structure. The antenna comprises one square shape and three circular shape patches to make it an MPTPS structure. One of the circular shapes' center is on the middle point of the upper side of the square patch. The other two circular patches' centers are on the middle point of the left and right side of the square patch. The Bottom side of the square patch is connected with the 50 Ω feed transmission line (TL). The back view of the antenna shows the partial ground plane (PGP) with its electronic band gap (EBG). Fig. 2 reveals the dimensions of the antenna which has been estimated and later optimized by (1)-(9) [12-16].

It is seen that the MPTPS antenna has an overall dimension of 25×40 mm^2 with a GP dimension of 17×18.9 mm^2 at the back of the antenna. The diameter of the each circle in the tree profile patch is 11 mm (radius, r = 5.5 mm) and the length of the sides of the square is same as the diameter of the circular shapes. The width of the 50 Ω feed TL is 1.24 mm and the length has been chosen as 20 mm as it is the one third of the free space wavelength (λ/3), where λ = 60 mm at center frequency 5 GHz, is the best optimized feed length for this design.

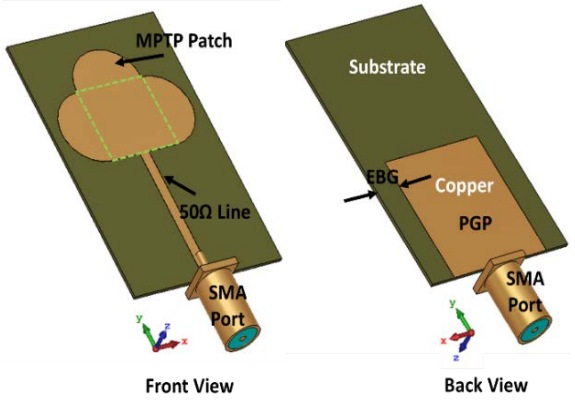

Fig. 1. The Front and the Back Geometry of the Proposed Single Element MPTPS Antenna.

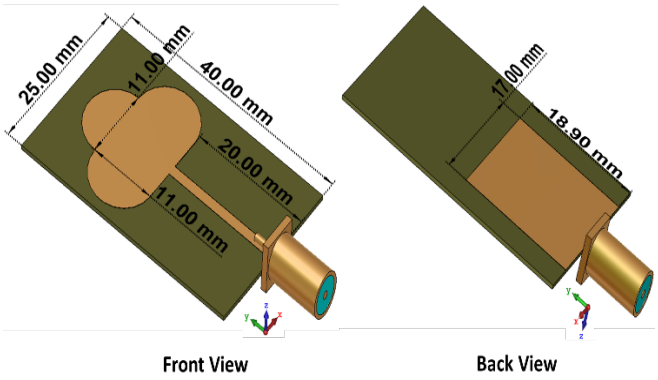

Fig. 2. The Detailed Dimension of the Proposed Antenna.

$$W = \frac{C_0}{2f_c\sqrt{\frac{(\varepsilon_r+1)}{2}}} \quad (1)$$

$$\varepsilon_e = \frac{\varepsilon_r+1}{2} + \frac{\varepsilon_r-1}{2}\left[1+12\frac{h}{W_p}\right]^{-\frac{1}{2}} \quad (2)$$

$$L_e = \frac{C_0}{2f_c\sqrt{\varepsilon_e}} \quad (3)$$

$$\Delta L = 0.412h\frac{(\varepsilon_e+0.3)(\frac{W_k}{h}+0.264)}{(\varepsilon_e-0.258)(\frac{W_k}{h}+0.8)} \quad (4)$$

$$L = L_e - 2\Delta L \quad (5)$$

$$L_g = 6h + L_k \quad (6)$$

$$W_g = W_g = 6h + W_k \quad (7)$$

$$r = \frac{F}{\left\{1+\frac{2h}{\pi\varepsilon_r F}\left[ln\left(\frac{\pi F}{2h}\right)+1.7726\right]\right\}^{\frac{1}{2}}} \quad (8)$$

$$F = \frac{8.791\times10^9}{f_c\sqrt{\varepsilon_r}} \quad (9)$$

Where, r is the radius of the circular patches. L and W are the length and the width of the any rectangular patch on the antenna. However, in this design, L = W since it's a square patch. The Lg and Wg are the length and width of the ground plane (GP) respectively. The substrate material for this proposed design is Rogers 3003 which has a dielectric constant (ε_r) of 3.00, the loss tangent ($tan\delta$) of 0.0019 and the substrate height (h) of 0.51 mm. After finalizing the single element design, the antenna has been used to be implemented for a 2 × 2 MIMO design configuration.

Fig. 3 shows the MIMO structure of the proposed array for smartphone. It can be seen from Fig. 3 that there are two pairs of antennas on the both side of the main board of the smartphone. Each pair has a combination of a 90^0 polarization diversity between them which actually give theoretically zero cross talk between them. The antenna 1 (A1) and antenna 2 (A2) is a pair and the other pair consists of antenna 3 (A3) and antenna 4 (A4). The total size of the main smartphone board is 145 × 75 mm^2 which represents the dimension of 5.5 inch display phone.

After this, in the MIMO configuration, a liquid crystal display (LCD) glass has been added to see the effect on the parameters (see Fig. 4). The material for the LCD is a lead glass which has a dielectric constant of 6, material density of 4200 kg/m^3, electrical conductivity of 1e-12 S/m and the thermal expansion coefficient of 8.18e-6 /K. The thickness of the LCD is chosen to be twice of the height of the substrate (1.1 mm) and the gap between the main board and the LCD is kept as 0.51 mm.

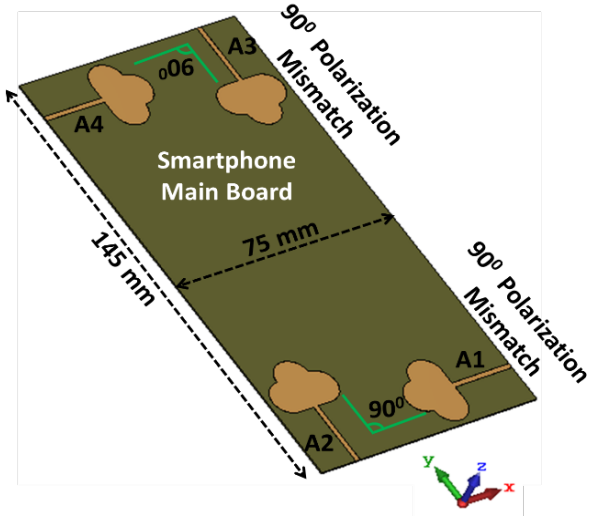

Fig. 3. The Proposed 2 × 2 MIMO Configuration for Smartphone.

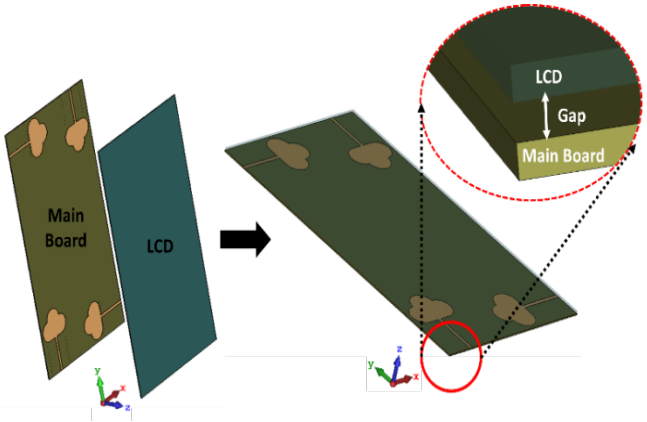

Fig. 4. MIMO Array with LCD.

Finally, to analyze the SAR performance of the antenna, a phantom model of hand tissue has been added to the structure. Fig. 5 represents the arrangement of the antenna with LCD and the added hand phantom. The simulation has been performed with the full 3-D electromagnetic simulator CST MWS 2021. In the next section all necessary result parameters and responses have been presented and analyzed.

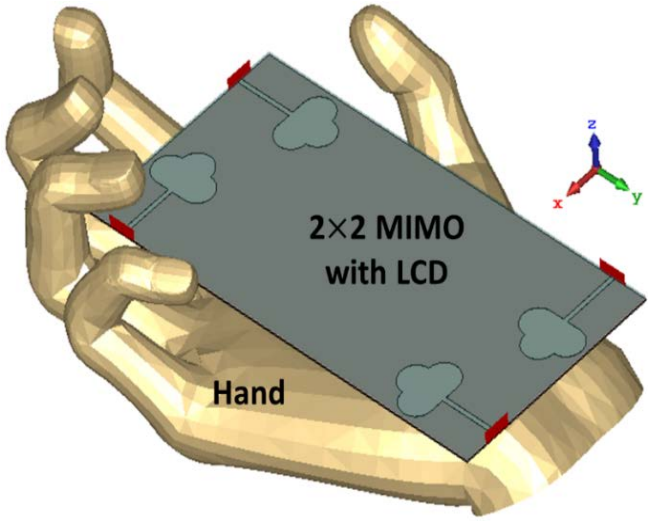

Fig. 5. MIMO Array with LCD and Hand Phantom.

IV. Result and Discussion

At first, the single element MPTPS antenna has been represented for analysis and discussion. Fig. 6 comprises the reference impedance (Fig. 6a), the S-parameter (S_{11}) (Fig. 6b) and the voltage standing ratio (VSWR) (Fig. 6c) of the antenna. In the beginning, it is important to see the impedance of the antenna. Since it is designed for a 50 Ω system, the reference impedance needs to be as close as 50 Ω value and from Fig. 6(a) it can be seen exactly the same as the impedance is 50 Ω throughout the BW. Now, to determine the working frequency BW it is necessary to check the S_{11} and the VSWR response of the antenna. From Fig. 6(b) it can be seen that the value $S_{11} \leq$ -10 dB starts from 2.83 GHz and stays below -10 dB until 7.16 GHz. So, it can be understood that the -10 dB BW is 4.33 GHz. To investigate further on the BW confirmation, the VSWR response has been analyzed. The condition VSWR ≤ 2 is commonly used to determine the working frequency of the antenna and it is seen from the Fig. 6(c) that the condition is satisfied from 2.81-7.23 GHz which increases the BW to 4.42 GHz.

Next, the efficiency, realized gain (RG) and the radiation pattern has been observed to assess the performance of the single MPTPS antenna. Fig. 7(a) and (b) comprise the radiation efficiency (RE) & total antenna efficiency (TAE), and the RG of the single MPTPS antenna respectively. Also, Fig. 8 comprises the 3-D and 2-D (polar) far-field radiation pattern at 3.5 GHz, 4.8GHz and 5.8 GHz. It can be seen from Fig. 7(a) that the RE and TAE both never go below 80% whereas goes as high as 96% at around 3 GHz. The realized gain (Fig. 7b) reveals that it reaches as high as 3.14 dBi which is very good considering the small size of the MPTPS antenna. Fig. 8(a), (c) and (e) comprise the 3-D far-field radiation pattern of the proposed MPTPS antenna at 3.5 GHz, 4.8 GHz and 5.8 GHz respectively. Furthermore, Fig. 8(b), (d) and (f) comprise the 2-D polar (the E- and H-plane) pattern of the antenna at those frequencies respectively. It can be seen that at all frequencies (from both 3-D and 2-D pattern) the far-field radiation pattern is bi-directional.

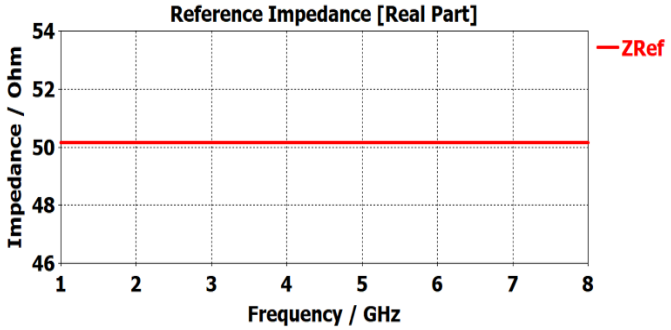

(a) Reference Impedance.

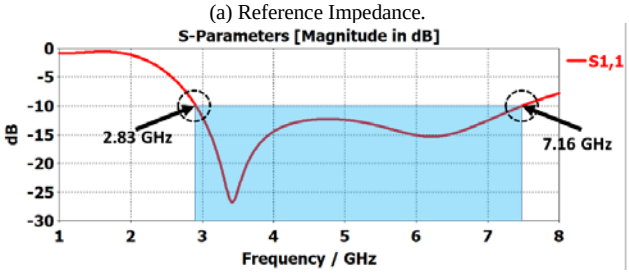

(b) S-Parameter (S_{11}).

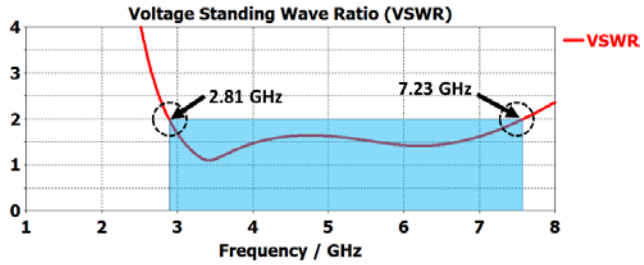

(c) VSWR.

Fig. 6. The (a) Reference Impedance, the (b) S-Parameter (S11) and the (c) VSWR of the Single Element MPTPS Antenna.

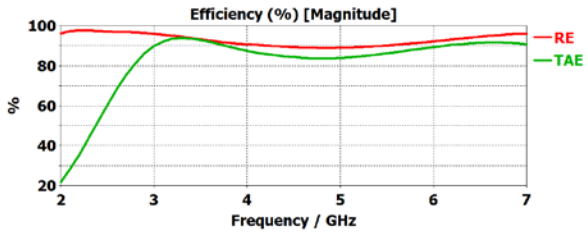

(a) RE and TAE of the MPTPS Antenna.

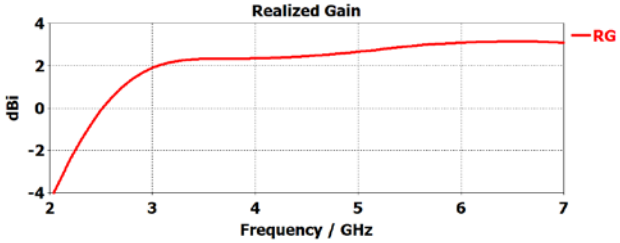

(b) Realized Gain of the MPTPS Antenna.

Fig. 7. Efficiencies and Realized Gain of the Single Element MPTPS Antenna.

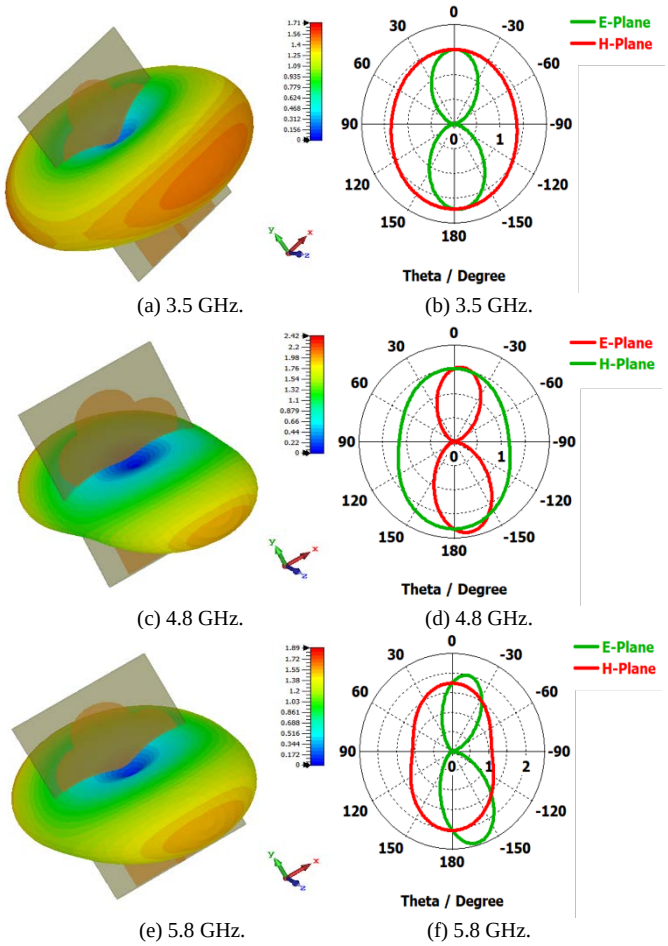

(a) 3.5 GHz. (b) 3.5 GHz.

(c) 4.8 GHz. (d) 4.8 GHz.

(e) 5.8 GHz. (f) 5.8 GHz.

Fig. 8. Far-Field Radiation Pattern at different Frequencies of the MPTPS Antenna.

After the confirmation of the performance assessment of the single element antenna, now, the next step is to investigate the performance of the proposed antenna in 2 × 2 MIMO configuration. Fig. 9(a) comprises the S-parameter's reflection parameter responses (S_{11}, S_{22}, S_{33} and S_{44}) of the four ports of the MIMO configuration. Similarly, Fig. 9(b) consists of the VSWR responses of the four different ports of the MIMO antenna. From both figures it can be seen that they are mostly same as the single element MPTPS antenna with a very little deviation. So, it is conclusive that in terms of the BW, the MIMO configuration keeps the working BW intact.

Fig. 10 illustrates the isolation between the ports which is one of the most important parameters to assess the performance of any MIMO array antenna. Since the array has two pairs of orthogonal configuration it is enough to investigate the port 1 and port 2 only. Fig. 10(a) comprises the S_{11}, S_{21}, S_{31} and S_{41} and Fig. 10(b) comprises the S_{12}, S_{22}, S_{32}, S_{42} and S_{34} to observe the isolations between different ports where S_{12}/S_{21} defines the isolation between port 1 and 2, S_{31} defines the isolation between and port 1 & 3, S_{41} defines the isolation between port 1 & 4 and S_{34} defines the isolation between port 3 & 4. Similarly, S_{32} and S_{42} defines the isolation between port 2 & 3 and port 2 & 4 respectively. It can be seen form both of the figure that except S_{42} (-21.1 dB), the rest of the isolation between different ports are below -30 dB. As the standard is less than -15 dB [6], this proposed MIMO exhibits an excellent isolation performance that is suitable for smartphones. Next, Fig. 11 comprises the surface current accumulation of the MIMO configuration at port 1 and port 2. It can be seen that due to the excitation at port 1 or port 2 other port does not accumulate much surface current and this is another justification on the good isolation between the ports in this MIMO configuration.

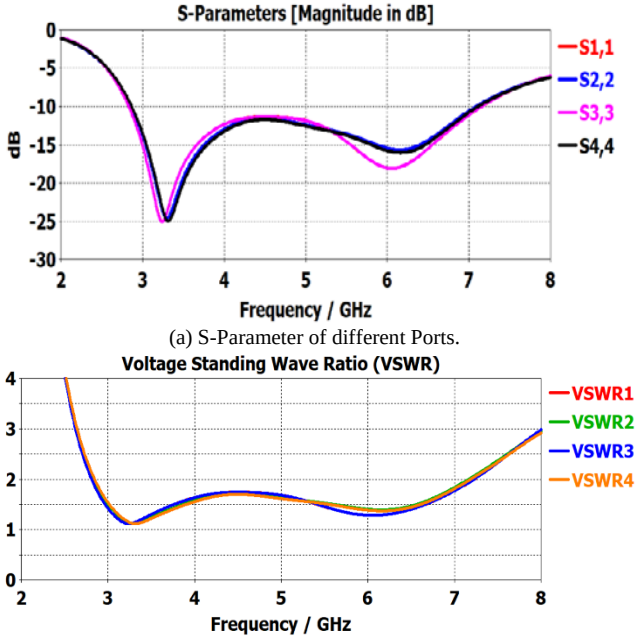

(a) S-Parameter of different Ports.

(b) VSWR of different Ports.

Fig. 9. (a) S-Parameters and (b) VSWRs of different Ports of the 2 × 2 MIMO Configuration.

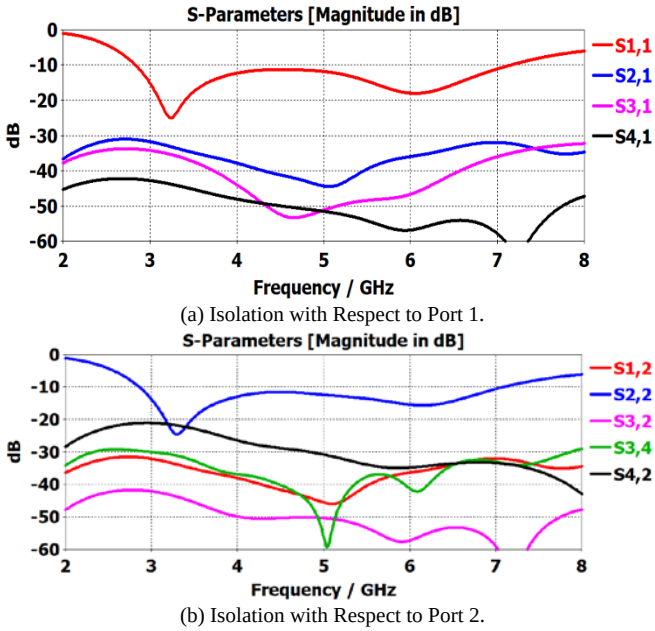

(a) Isolation with Respect to Port 1.

(b) Isolation with Respect to Port 2.

Fig. 10. Isolation between different Ports of the MIMO.

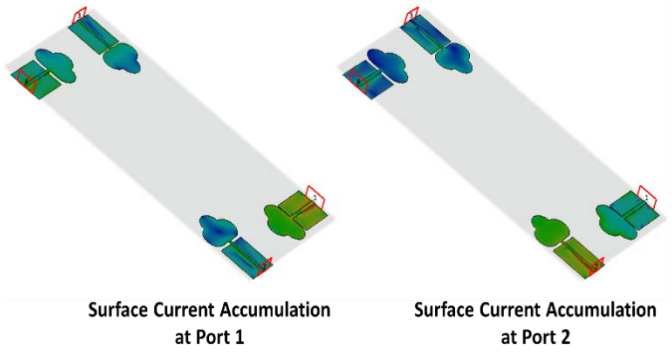

Fig. 11. Surface Current Accumulation at different Ports.

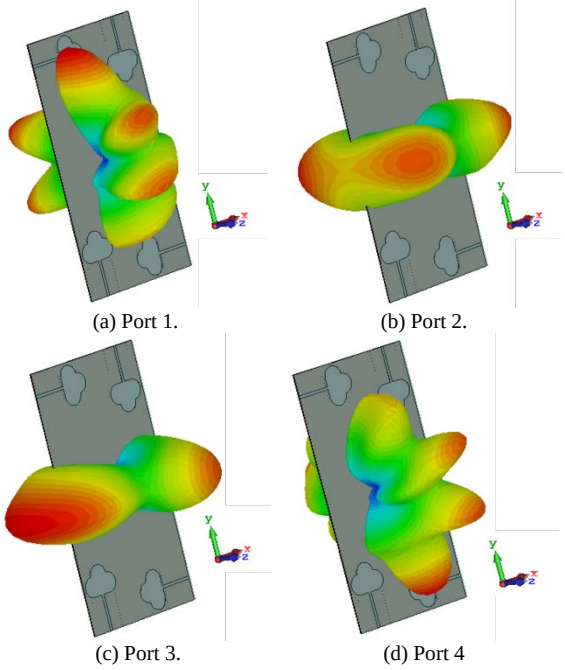

(a) Port 1. (b) Port 2.

(c) Port 3. (d) Port 4

Fig. 12. 3-D Radiation Pattern for different Ports at 3.5 GHz.

The 3-D radiation patterns at 3.5 GHz in different ports can be seen in Fig. 12. The pattern at port 1 and 4 exhibit the front and back side radiating nature. On the other hand, port 2 and port 3 exhibit the radiation pattern at the right and left sides of the main board of the smartphone. So, it apparent that the combination of the four ports together covers all four directions of the radiation which makes this proposed configuration suitable for this specific application. As the assessment of the isolation and radiation performance is done, it is crucial to observe and analyze the other parameters such as the combined RG, the ECC and the DG of the array. Fig. 13(a), (b) and (c) discloses those parameters respectively. Since it's a four port MIMO, there will be three ECCs (ECC_{12}, ECC_{13} & ECC_{14}) and three DGs (DG_{e12}, DG_{e13} & DG_{e14}). The ECC for different forts can be calculated by (10)-(12) and similarly the DG can be estimated by (13)-(15) [17].

$$ECC_{12} = \frac{|S_{11}^{*}S_{12}+S_{12}^{*}S_{22}+S_{13}^{*}S_{32}+S_{14}^{*}S_{42}|^2}{(1-(|S_{11}|^2+|S_{12}|^2)+(|S_{13}|^2+|S_{14}|^2))^2} \quad (10)$$

$$ECC_{13} = \frac{|S_{11}^{*}S_{13}+S_{12}^{*}S_{23}+S_{13}^{*}S_{33}+S_{14}^{*}S_{43}|^2}{(1-(|S_{11}|^2+|S_{12}|^2)+(|S_{13}|^2+|S_{14}|^2))^2} \quad (11)$$

$$ECC_{14} = \frac{|S_{11}^{*}S_{14}+S_{12}^{*}S_{24}+S_{13}^{*}S_{34}+S_{14}^{*}S_{44}|^2}{(1-(|S_{11}|^2+|S_{12}|^2)+(|S_{13}|^2+|S_{14}|^2))^2} \quad (12)$$

$$DG_{e12} = 10\sqrt{1-|ECC_{12}|^2} \quad (13)$$

$$DG_{e13} = 10\sqrt{1-|ECC_{13}|^2} \quad (14)$$

$$DG_{e14} = 10\sqrt{1-|ECC_{14}|^2} \quad (15)$$

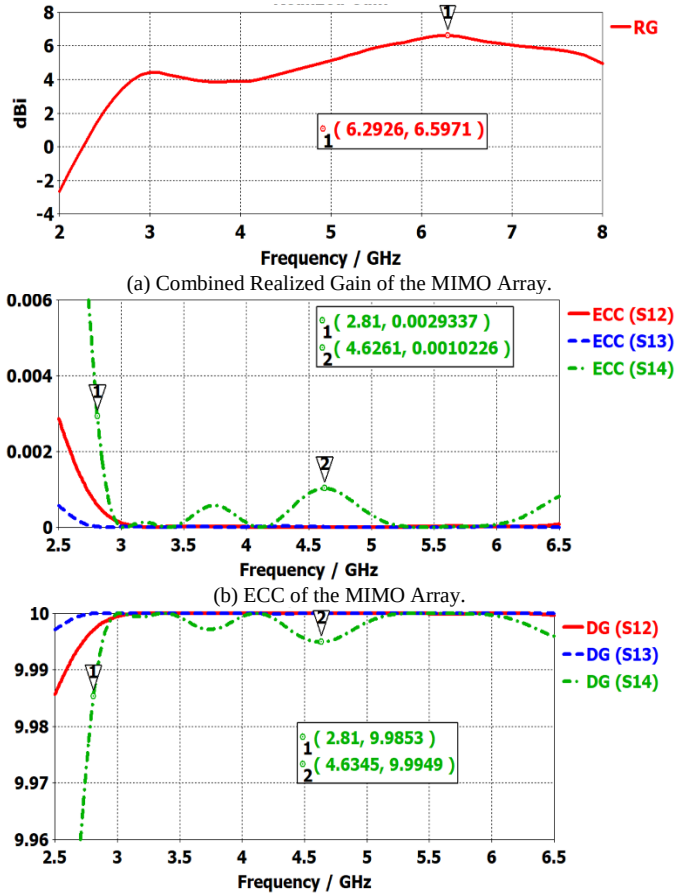

(a) Combined Realized Gain of the MIMO Array.

(b) ECC of the MIMO Array.

(c) Diversity Gain of the MIMO Array.

Fig. 13. The (a) Realized Gain, (b) ECC and (c) Diversity Gain of the MIMO Array.

The combined RG of the MIMO array (seen in Fig. 13a) never goes below 4 dBi throughout the entire BW of operation, whereas, it goes as high as 6.6 dBi around 6.3 GHz. From 3 to 6 GHz the RG stays between 4-6 dBi. From Fig. 13(b), the ECCs of the array can be observed. A lower value of ECC indicates the good isolation among the radiating elements of any MIMO array structure. It can be seen that throughout the whole BW the value starts with 0.0029 at 2.81 GHz and in most of the BW, it never goes higher than 0.001. As the standard for ECC should be less than 0.3 [17], it can be concluded that the value of the ECC for this proposed MIMO array is excellent. Similarly, the DG responses seen from Fig. 13(c), are also in agreement with the ECC responses, staying higher than the value of 9.9978 throughout the BW. Whereby most of the working BW is more than 9.9949. Lastly, the SAR values are illustrated in Fig. 14(a), (b) and (c) for 3.5 GHz, 4.8 GHz and 5.8 GHz, respectively. The SAR measures the amount of radiation energy would dissipated into a human

body. So, the value is desired to be keep as low as possible as the higher radiated power may harm human tissue. As long as the SAR value is below standard specification, any design can be acceptable for human body proximity centric applications such as smartphones. The standard of the SAR value is SAR < 2 W/Kg for 10g mass [11]. At 3.5 GHz, it is seen that the SAR value is very low dropping at 0.887641 W/Kg which is remarkable. Similarly, at 4.8 GH it increases a little up to 0.90636 W/Kg and at 5.8 GHz the value goes to 0.950047 W/Kg. With these SAR results it is conclusive that the proposed design is not harmful for human body and well below within the acceptable standard value of SAR.

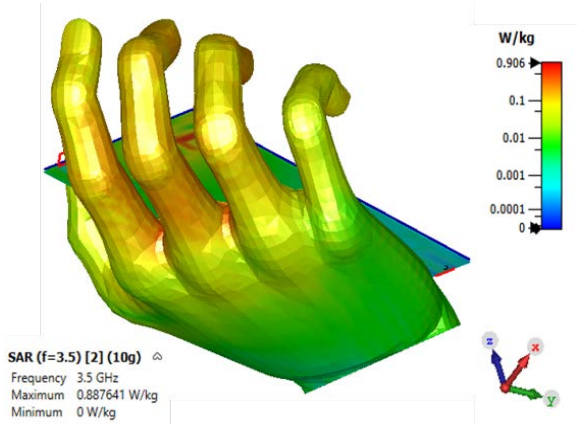

(a) SAR at 3.5 GHz.

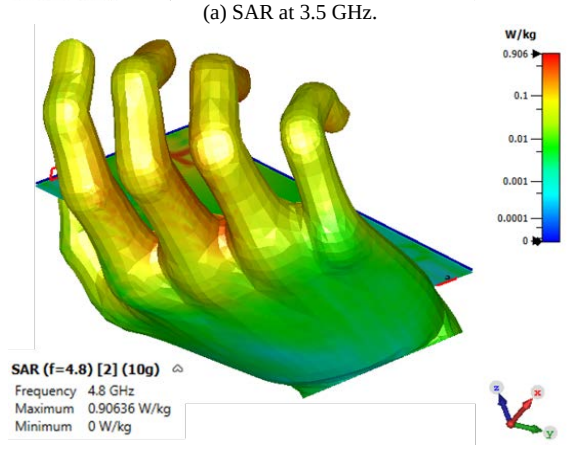

(b) SAR at 4.8 GHz.

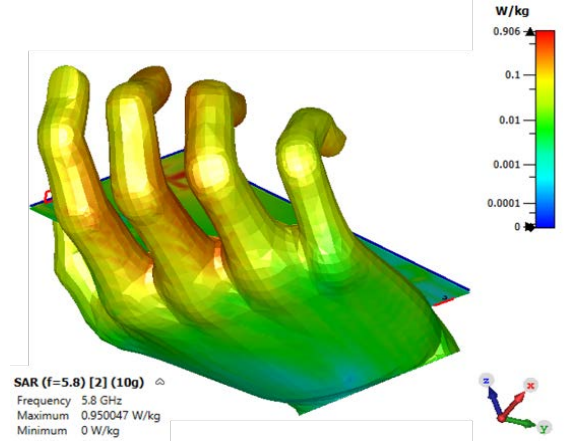

(c) SAR at 5.8 GHz.

Fig. 14. The SAR Values for (a) 3.5 GHz, (b) 4.8 GHz and 5.8 GHz.

V. Conclusion

The MPTPS single antenna has been presented here. The antenna working frequency is between 2.81 – 7.26 GHz covering all the 5G NR 77/78 and 79 bands for mobile communication. The antenna has a bi-directional radiation pattern and single antenna gain is up 3.14 dBi. Also, the antenna efficiency is good around 96% and it never goes below 80% throughout the BW of the antenna. Later, the proposed antenna has implemented in a 2×2 MIMO configuration of 2 pairs with the polarization diversity of 90^0 between the elements of the each pair. A good isolation of more than -30 dB is observed between the port except between port 2 and 4 where it drops as low as -21.1 dB which is still better that the existing antennas for smartphones. The MIMO configuration has a good far-field radiation pattern with covering all four directions together with four ports. The combined RG is up to 6.6 dBi. The ECC is as low as 0.0029 and mostly stays below 0.001 throughout the BW. Similarly, the DG responses of the MIMO configuration are also mostly below 9.9949 throughout the entire BW. One more aspect of this array is the SAR (10g) value. It is remarkably very low at 3.5 GHz with a value of 0.887641 W/Kg which is far below than the acceptable standard value of 2.0 W/Kg indicating the safeness for its application around human body proximity centric applications. The future aspect of this research is realized and validates this proposed design in the real world environment through experimentation. This design will motivate the antenna engineers to design a highly isolated and efficient MIMO array antenna for smartphone applications.

Acknowledgment

This work has been funded by the grant PJP/2020/FTKEE/PP/S01753 from the center for research and innovation management (CRIM), University Teknikal Malaysia Melaka (UTeM).

References

[1] Pant, A., Singh, M., & Parihar, M. S. (2021). A frequency reconfigurable/switchable MIMO antenna for LTE and early 5G applications. AEU - International Journal of Electronics and Communications, 131 doi:10.1016/j.aeue.2021.153638.

[2] https://fccid.io/frequency-explorer.php. Last accessed on 30th May 30, 2021.

[3] Guo, J., Cui, L., Li, C., & Sun, B. (2018). Side-edge frame printed eight-port dual-band antenna array for 5G smartphone applications. IEEE Transactions on Antennas and Propagation, 66(12), 7412-7417. doi:10.1109/TAP.2018.2872130.

[4] Li, G., Zhai, H., Ma, Z., Liang, C., Yu, R., & Liu, S. (2014). Isolation-improved dual-band MIMO antenna array for LTE/WiMAX mobile terminals. IEEE Antennas and Wireless Propagation Letters, 13, 1128-1131. doi:10.1109/LAWP.2014.2330065.

[5] Kumar, N., & Khanna, R. (2021). A two element MIMO antenna for sub-6 GHz and mmWave 5G systems using characteristics mode analysis. Microwave and Optical Technology Letters, 63(2), 587-595. doi:10.1002/mop.32626.

[6] Kulkarni, J., Desai, A., & Sim, C. -. D. (2021). Wideband four-port MIMO antenna array with high isolation for future wireless systems. AEU - International Journal of Electronics and Communications, 128 doi:10.1016/j.aeue.2020.153507.

[7] Huang, J., Dong, G., Cai, J., Li, H., & Liu, G. (2021). A quad-port dual-band mimo antenna array for 5g smartphone applications. Electronics (Switzerland), 10(5), 1-9. doi:10.3390/electronics10050542.

[8] Jamshed, M. A., Ur-Rehman, M., Frnda, J., Althuwayb, A. A., Nauman, A., & Cengiz, K. (2021). Dual band and dual diversity four-element mimo dipole for 5G handsets. Sensors (Switzerland), 21(3), 1-13. doi:10.3390/s21030767.

[9] Lee, C. & Su, S. (2021). Decoupled multi-input multi-output antennas with a common dipole for wideband 5G laptop computers. Microwave and Optical Technology Letters, 63(4), 1286-1293. doi:10.1002/mop.32736.

[10] Kiani, S. H., Altaf, A., Abdullah, M., Muhammad, F., Shoaib, N., Anjum, M. R., Damasevicius, R., Blažauskas, T. (2020). Eight element side edged framed MIMO antenna array for future 5G smart phones. Micromachines, 11(11). doi:10.3390/mi11110956.

[11] Serghiou, D., Khalily, M., Singh, V., Araghi, A., & Tafazolli, R. (2020). Sub-6 GHz dual-band 8 × 8 MIMO antenna for 5G smartphones. IEEE Antennas and Wireless Propagation Letters, 19(9), 1546-1550. doi:10.1109/LAWP.2020.3008962.

[12] Islam, M. S., Ibrahimy, M. I., Motakabber, S. M. A., & Hossain, A. Z. (2018, September). A Rectangular Inset-Fed Patch Antenna with Defected Ground Structure for ISM Band. In 2018 7th International Conference on Computer and Communication Engineering (ICCCE) (pp. 104-108). IEEE. doi:10.1109/ICCCE.2018.8539260.

[13] Zakir Hossain, A. K. M., Hassim, N. B., Alsayaydeh, J. A. J., Hasan, M. K., & Islam, M. R. (2021). A tree-profile shape ultra wide band antenna for chipless RFID tags. International Journal of Advanced Computer Science and Applications, 12(4), 546-550. doi:10.14569/IJACSA.2021.0120469.

[14] Azam, S. M. K., Islam, M. S., Hossain, A. K. M. Z., & Othman, M. (2020). Monopole antenna on transparent substrate and rectifier for energy harvesting applications in 5G. International Journal of Advanced Computer Science and Applications, 11(8), 84-89. doi:10.14569/IJACSA.2020.0110812.

[15] Zakir Hossain, A. K. M., Hassim, N. B., Kayser Azam, S. M., Islam, M. S., & Hasan, M. K. (2020). A planar antenna on flexible substrate for future 5g energy harvesting in malaysia. International Journal of Advanced Computer Science and Applications, 11(10), 151-155. doi:10.14569/IJACSA.2020.0111020.

[16] Zakir Hossain, A. K. M., Indra, W. A., Jamil Alsayaydeh, J. A., & Herawan, S. G. (2021). A planar monopole UWB antenna with partial ground plane for retransmission-based chipless RFID. International Journal of Intelligent Engineering and Systems, 14(4), 539-547. doi:10.22266/ijies2021.0831.47.

[17] Elfergani, I.; Iqbal, A.; Zebiri, C.; Basir, A.; Rodriguez, J.; Sajedin, M.; Pereira, A.d.O.; Mshwat, W.; Abd-Alhameed, R.; Ullah, S. (2020). Low-profile and closely spaced four-element mimo antenna for wireless body area networks. Electronics (Switzerland), 9(2) doi:10.3390/electronics9020258.